SUPPLEMENTARY MATERIAL

Paper-based sample processing for fast and direct MS analysis of multiple analytes from serum samples

Fu Zhang,‡[a] Bin Ji,‡[b] Xiang-Hong Yan,[a] Shuang Lv,[a] Fang Fang,[a] Shuang Zhao,[a]

Xiao-Lin Guo [b] and Zhi-Yong Wu [a]*

[a] Chemistry Department, College of Sciences, Northeastern University, Shenyang 110819, China

[b] The First Affiliated Hospital of China Medical University, Shenyang, 110001, China

‡ The two authors contribute equally

*Correspondence to: Zhi-Yong Wu, Dr & Prof.

Email: zywu@mail.neu.edu.cn

Tel/Fax: +86 (0)2483687659

Supporting Information Sections:

Section 1. The pI value, mass-spectrometric conditions, stock solution concentration levels of AAs and their isotopic IS

The MS determination is performed based flow injection analysis format. All samples were analyzed on an API 4000 tandem triple-quadrupole mass spectrometer (AB SCIEX, USA). The ion spray voltage, temperature, curtain gas, gas1, and gas2 were set at 5500 V, 550° C, 20L/min, 10L/min, and 10L/min, respectively.

Table S1 The conditions of amino acids and their isotopic internal standards

AA	pI	Molecular Formula	Molecular weight	Isotope labeled AA molecular formula	Isotope labeling of AA molecular weight	Stock solution concentration level（μmol/mL）
Glycine /Gly	5.97	$C_2H_5NO_2$	75.07	^{15}N,2-^{13}C-$C_2H_5NO_2$	77.07	2.5
Alanine /Ala	6.00	$C_3H_7NO_2$	89.10	$^{2}H_4$-$C_3H_7NO_2$	93.10	0.5
Valine /Val	5.98	$C_5H_{11}NO_2$	117.15	$^{2}H_8$-$C_5H_{11}NO_2$	125.15	0.5
Leucine /Leu	5.98	$C_6H_{13}NO_2$	131.17	$^{2}H_3$-$C_6H_{13}NO_2$	134.17	0.5
Methionine /Met	5.74	$C_5H_{11}NO_2S$	149.21	$^{2}H_3$-$C_5H_{11}NO_2S$	152.21	0.5
Phenylalanine /Phe	5.48	$C_9H_{11}NO_2$	165.19	$^{13}C_6$-$C_9H_{11}NO_2$	171.19	0.5
Tyrosine/Tyr	5.66	$C_9H_{11}NO_3$	181.19	$^{13}C_6$-$C_9H_{11}NO_3$	187.19	0.5
Ornithine·HCl/Orn·HCl	10.00	$C_5H_{12}N_2O_2$·HCl	168.62	$^{2}H_6$-$C_5H_{12}N_2O_2$·HCl	174.62	0.5
Citrulline /Cit	5.92	$C_6H_{13}N_3O_3$	175.19	$^{2}H_2$-$C_6H_{13}N_3O_3$	177.19	0.5
Arginine·HCl/Arg·HCl	10.76	$C_6H_{14}N_4O_2$·HCl	210.66	$^{2}H_4$,^{13}C-$C_6H_{14}N_4O_2$·HCl	215.66	0.5
Proline /Pro	6.30	$C_5H_9NO_2$	115.13	$^{13}C_5$-$C_5H_9NO_2$	120.13	0.5

Table S2 MRM characteristic ions and MS conditions

	AA	Q1 Mass(Da)	Q3 Mass(Da)	DP (Volts)	CE (Volts)	Time (msec)
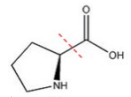	Pro	116.100	70.100	50.000	23.000	25.0
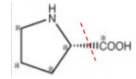	Pro IS	121.100	74.100	50.000	23.000	25.0
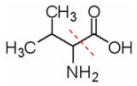	Val	118.200	72.200	45.000	17.000	25.0
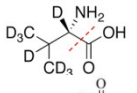	Val IS	126.200	80.200	45.000	17.000	25.0
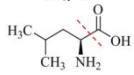	Leu	132.300	86.000	40.000	15.000	25.0
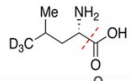	Leu IS	135.300	89.000	40.000	15.000	25.0
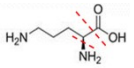	Orn	133.200	70.000	35.000	25.000	25.0
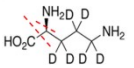	Orn IS	139.200	76.000	35.000	25.000	25.0
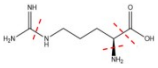	Arg	175.200	70.000	55.000	37.000	25.0
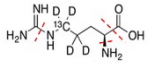	Arg IS	180.200	75.000	55.000	37.000	25.0
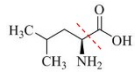	Met	150.200	103.900	45.000	14.000	25.0
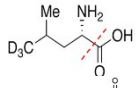	Met IS	153.200	106.900	45.000	14.000	25.0
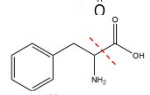	Phe	166.300	120.000	37.000	17.000	25.0
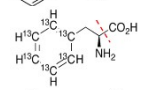	Phe IS	172.300	126.000	37.000	17.000	25.0
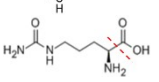	Cit	176.200	113.000	35.000	22.000	25.0
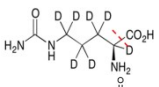	Cit IS	178.200	115.000	35.000	22.000	25.0
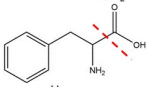	Tyr	182.100	136.100	40.000	18.000	25.0
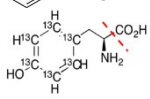	Tyr IS	188.100	142.100	40.000	18.000	25.0

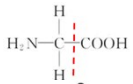	Gly	76.000	30.100	37.000	16.000	25.0
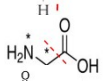	Gly IS	78.000	32.100	37.000	16.000	25.0
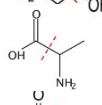	Ala	90.100	44.100	35.000	15.000	25.0
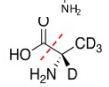	Ala IS	94.100	48.100	35.000	15.000	25.0

Section 2. Chromogenic localization of amino acids

After electrical treatment with PAD, the paper channel was transferred to a glass slide placed on a heating plate and a drop of ninhydrin solution was added for specific color development of amino acids (violet-blue for most amino acids, yellow for proline and hydroxyproline).

Section 3. Preparation of isotope spiking sample

To examine the differences between different sample preparation methods, sample solutions prepared with extract solution and deionized water were subjected to MS detection after PAD electrolysis. 20 μL isotope IS working solution and 60 μL extraction solution (or deionized water) were added to 60 μL serum sample, vortex and stored at 4°C. The spiked serum samples prepared as above contained 3 μL serum per 7 μL. As shown in Table S3, different solution preparation methods affected the reproducibility of the individual amino acid detection results. Based on the above, the extract solution was finally used for spiking in all subsequent experiments.

Table S3 RSD comparison of MS results with different spiked sample preparation methods

	Methanol preparation	Deionized water preparation
AA	RSD	RSD
Ala	0.92%	2.28%
Gly	1.25%	1.34%
Pro	0.94%	0.42%
Leu	1.78%	0.96%
Val	1.01%	0.16%
Met	2.42%	1.53%
Phe	1.28%	0.50%

Tyr	1.20%	0.86%
Cit	1.81%	3.80%
Orn	1.67%	2.87%
Arg	1.88%	3.72%

Note: The data above are all MSMS assay results of the sample direct extraction method. Due to the large difference in storage time of spiked samples (spanning about two months) and different preparation methods, it is difficult to compare the measured values, and only the RSD cases are compared here to examine the trend changes. N=4

Section 4. Optimization of electrolytes supported

We also compared the buffer-inhibitor system with the acid-base uninhibited system in terms of the accumulation of samples on the channels, as shown in Figure S1. In conventional buffer systems, amino acids cannot migrate well to the channels when the samples are loaded as DBS. Due to the fact that electroosmotic flow is suppressed in this system and electromigration alone is not sufficient to migrate amino acids from the DBS to the paper channels, as well as demonstrates the importance of the presence of an appropriately sized electroosmotic flow in the system. In the established acid-base system, both loading methods can obtain stable stacking bands, and the acid-base system can well form a sharp pH gradient on the paper channel to stack the amphiphiles with pI in a certain area, thus, the acid-base uninhibited system was used in this study.

Table S4 pH and conductivity of supported electrolyte solutions

Support electrolyte system		pH	Conductivity μs/cm
Acid-base system	10 mM $NH_3•H_2O$	10.7	116.9
	10 mM HAc	2.6	368
Buffer-inhibitor system	10 mM $NH_3•H_2O$ - NH_4Ac	9.8	523
	10 mM HAc - NH_4Ac(0.1% HEC)	4.3	650

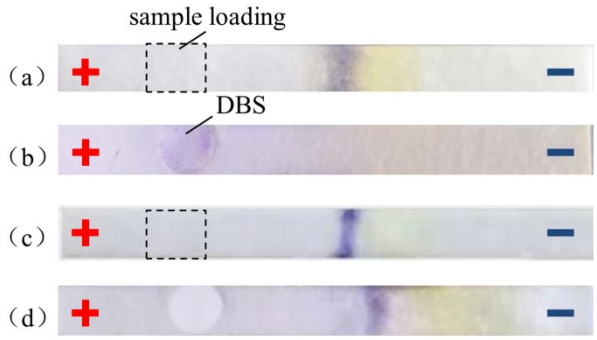

Figure S1. AA stacking effect graphs. (a) and (b) showed the effect of loading sample solution and DBS for the buffer-inhibitor system; (c) and (d) showed the effect of loading sample solution and sample piece for the acid-base system.

Section 5. Characterization of electroosmotic flow

In EFGF, the electroosmotic flow needs to be regulated to meet the needs. In this system, the EOF points from the positive pole to the negative pole. The sample is loaded on the anodic channel, where the pH < pI, the amino acids are positively charged and migrate towards the negative pole under the influence of Ep and EOF; when they migrating near the pH = pI position, the amino acids stop migrating and accumulate there.

The intensity of electroosmotic flow in the system was examined with the aid of colored rhodamine B (an electrically neutral substance). The entire paper-based fluid channel was first wetted with 20 μL HAc solution (excluded capillary action), then 400 μL of HAc solution containing 0.4 mg/mL rhodamine B was added to the anode reservoir and 400 μL of $NH_3•H_2O$ solution was added to the cathode reservoir and treated with electricity at 200 V. The electroosmotic trickle is estimated based on the time and distance of rhodamine B movement. The electroosmotic flow under different paper materials and different systems are shown in Figure S2. The results showed that the EOF can be effectively inhibited by adding inhibitors, and the EOF of glass fiber paper-based under buffer system is significant (dripping degree $6.84*10^{-4}cm^2V^{-1}s^{-1}$), and the EOF dripping degree of glass fiber under the acid-base system is slightly larger than that of quartz fiber paper-based, $4.05*10^{-4}cm^2V^{-1}s^{-1}$ and $2.20*10^{-4}cm^2V^{-1}s^{-1}$, respectively.

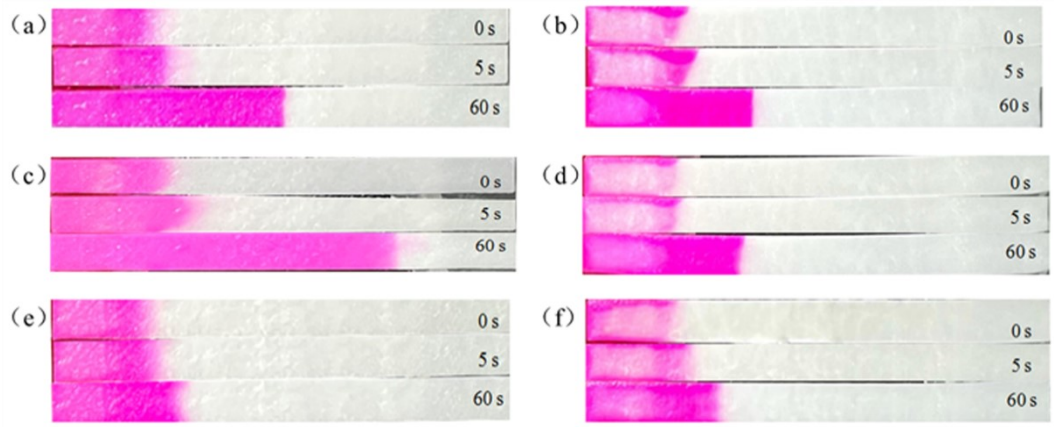

Figure S2 Characterization of electroosmotic flow. (a) and (b) are glass fiber filter paper and quartz fiber filter paper in the acid-base system; (c) and (d) are glass fiber filter paper and quartz fiber filter paper in the buffered system; (e) and (f) are glass fiber filter paper and quartz fiber filter paper in buffered-inhibited system, respectively.

Section 6. Optimization of paper-based materials

The paper-based materials used in the system were selected and optimized. Figure S3a shows the effect of amino acids stacking when different paper materials were used after PAD treatment. The order from top to bottom in Figure S3a is K-49 glass fiber membrane, quartz fiber membrane, Whatman NO.1, nitrocellulose membrane and cellulose acetate membrane. Among them, on Whatman NO.1 and nitrocellulose membranes, amino acids in serum cannot accumulate well into bands. On the cellulose acetate membrane, amino acids can accumulate into bands. However, the cellulose acetate membrane is poorly hydrophilic, the channel is not easily wetted and has a low water absorption rate, making them prone to "steam drying" during the process. As for the glass fiber membrane and quartz fiber membrane, both of them can form stable stacking bands on the channels. To further investigate the performance of both of them, the MS of amino acids treated based on both materials were examined separately, as shown in Table S3b. The overall RSD of the glass fiber membrane is lower than that of the quartz fiber membrane, thus the glass fiber membrane was chosen for the subsequent experiments.

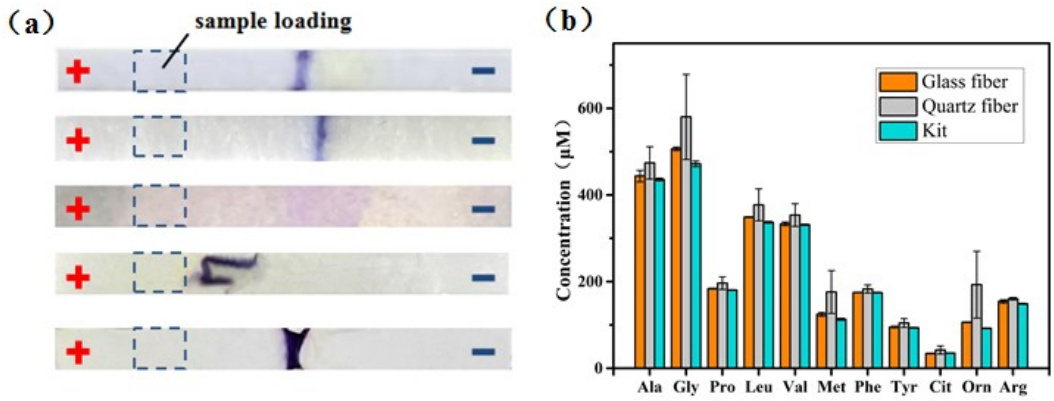

Figure S3 (a) Selection of paper-based materials, from top to bottom: K-49 glass fiber membrane, quartz fiber membrane, Whatman NO.1, nitrocellulose membrane and cellulose acetate membrane; (b) Results of MS assay with glass fiber membrane and quartz fiber membrane PAD treatment. N=6

Section 7. Optimization of PAD loading position

We also examined the MS detection of AAs when the samples were loaded at different positions, as shown in Figure S4. The results showed that the mean values of the assay results were relatively close between the two loading positions, but with slightly different precision. Loading in the anodic region was more effective, with RSDs below 4% for all 11 AAs, so the anodic region was chosen for loading in all subsequent experiments.

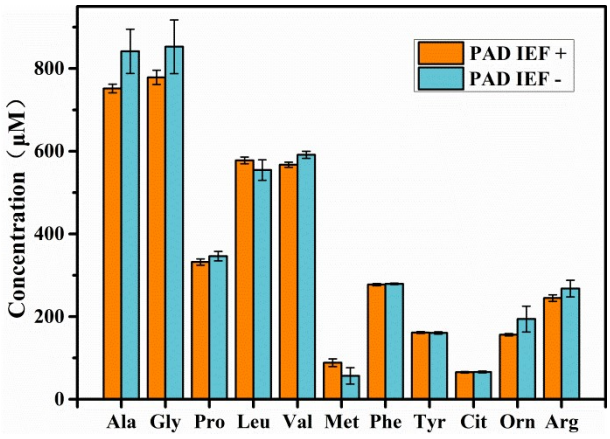

Figure S4. MS detection results for AAs at different sample loading positions. N=6。

Section 8. Optimization of PAD sample wetting and extraction methods

For liquid samples, PAD IEF processing can be performed directly. For the DBS or PAD dry sample spots, they need to be wetted with the solution before treatment. We compared the results of 1:1 methanol aqueous solution wetting and deionized water

wetting (Figure S5a) and found that although the mean values of the assay results were similar, the precision of the effect was better with water wetting. Therefore, deionized water was used to wet the dried samples in the experiments.

Extraction from the stacking zone after PAD treatment is also a necessary step to perform off-line MS determination. For this purpose, we compared the results of simple (laboratory method) and high intensity leaching (Kit method) assays (Figure S5b). The results showed that both leaching methods give approximately the same results, except for Ala where good precision (RSD less than 4 %) was obtained.

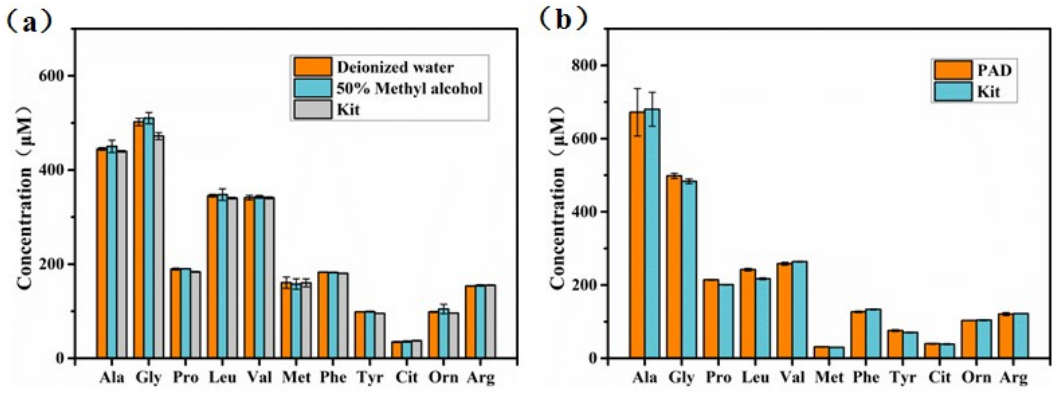

Figure S5. Comparison plots of MS/MS determination mean values. (a) Different wetting conditions; (b) Different post-treatment methods. N=4

Section 9. Application to healthy and pathological samples MS determination.

Comparing the difference in MS assay results between the PAD method and the Kit method for AAs in healthy serum samples and pathological serum samples, Figure S6 demonstrated that the difference characteristics determined by the two methods showed the same trend.

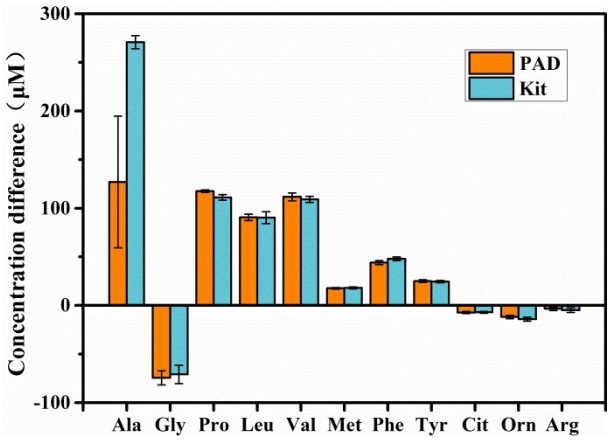

Figure S6 Difference in MS detection between healthy and pathological samples